Design of a Millimeter-Wave CMOS Radiation Oscillator With an Above-Chip Patch Antenna

Mamoru Sasaki

***Abstract*—This brief presents a design method of a millimeter-wave CMOS radiation oscillator for broadband short-range communication. An above-chip patch antenna is proposed for the radiation oscillator. The proposed antenna has a balanced port, which makes it suitable for the direct connection of CMOS cross-coupling transistors. The properties of the antenna are analyzed by an electromagnetic field solver, and, in particular, the input resistance is discussed in detail, so that the condition of millimeter-wave oscillation is satisfied even by CMOS FETs having gains lower than GaAs FETs. Furthermore, on/off-keying modulation can be carried out using switch transistors, and two switching techniques are used to realize a large data rate. A performance of 500 Mb/s and a total efficiency of 0.12, which includes both the antenna and the circuit efficiencies, are confirmed by circuit simulation.**

***Index Terms*—Balanced structure, broadband communication, CMOS integrated circuit, microstrip patch antenna, millimeter-wave, radiation oscillator, short-range communication.**

I. Introduction

One of interesting fields of application of millimeter-wave communication is broadband short-range communication, e.g., personal area network and wireless connection among personal equipment [1]. Compared with microwave-based systems, millimeter-wave-based systems offer the following advantages:

1) availability of broader frequency bands;
2) antennas of smaller dimensions;
3) smaller and lower weight equipment;
4) short wavelength may prevent interference between communication systems since the attenuation over a fixed distance is inversely proportion to the wavelength.

The use of millimeter-wave-based systems is extremely common for the above applications. The requirements for these applications are monolithic integration of the millimeter-wave front-end and application circuits via standard CMOS technology. Furthermore, these applications also require low power consumption for portable use.

A number of studies have examined the above IC integration technique [2], [3]. The design of wireless circuits, including the above IC resonators and filters, has enabled highly integrated transceiver architectures. Moreover, aggressive scaling CMOS technology has enabled the fabrication of highly integrated CMOS millimeter-wave circuits for data communication applications [4], [5].

In this brief, a millimeter-wave CMOS radiation oscillator is designed by employing an above-chip microstrip patch antenna. The radiation oscillator is a circuit block that combines an oscillator and an antenna by using the antenna structure as the resonator of the oscillator. This facilitates a small circuit layout and avoids losses between the oscillator and the antenna. Furthermore, the oscillator can also function as a transmitter because it enables on/off-keying modulation.

II. Above-Chip Patch Antenna

A. Antenna Structure

The structure of the above-chip patch antenna is illustrated in Fig. 1. The dielectric layer and the patch antenna are stacked above the CMOS chip by postprocess assembly. The top metal layer in CMOS technology forms the ground plane for the patch antenna. The top metal ground plane can shield other CMOS application circuits below it against electromagnetic interference from the microstrip patch antenna. The patch antenna is fed by electromagnetic couplings from slots carved in the ground plane. The feed method makes the postprocess assembly very easy because no via-hole process is needed in the dielectric layer. The detailed shape of the slots is shown in Fig. 2. These two slots allow the symmetric structure to realize a balanced input and can be applied for cross-coupled oscillators with CMOS devices [6]. The rectangles protruding into the slots form a MOSFET array that composes a cross-coupled transistor pair. The layout pattern will be detailed later herein.

The planar structure allows extremely small dimensions, avoiding losses in the feed-line between the oscillator and the antenna. Furthermore, the direct connection without a feed-line makes it possible to design the input impedance of the antenna independent of the feed-line characteristic impedance. Here, we try to design a large antenna impedance to realize a millimeter-wave radiation oscillator by CMOS cross-coupled transistors. The conductance of the CMOS cross-coupled transistors compensates the loss of the antenna impedance, and the (negative) conductance $G_{\rm cir}$ is

$$G_{\rm cir} = -g_{\rm mN} - g_{\rm mP}$$

where $g_{\rm mN}$ and $g_{\rm mP}$ are the transconductances of the nMOS FET and PMOSFET, respectively. If the antenna impedance is low, then a large number of fingers of the transistor are needed to compensate for the large loss of the input impedance. However, the large number of fingers reduces the oscillation frequency as

Manuscript received November 24, 2005; revised April 8, 2006. This work was supported in part by the Ministry of Education, Science, Sports and Culture under a Grant-in-Aid for Scientific Research (B), 2005, 17360167 This paper was recommended by Associate Editor P. P. Sotiriadis.

The author is with the Graduate School, Hiroshima University, Hiroshima 739-8530, Japan (e-mail: sasaki@dsl.hiroshima-u.ac.jp).

Digital Object Identifier 10.1109/TCSII.2006.882234

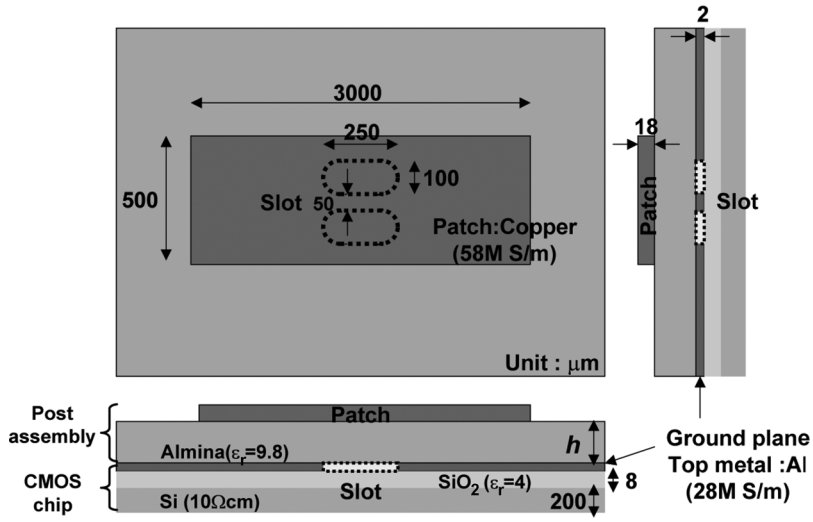

Fig. 1. Structure of the above-chip patch antenna.

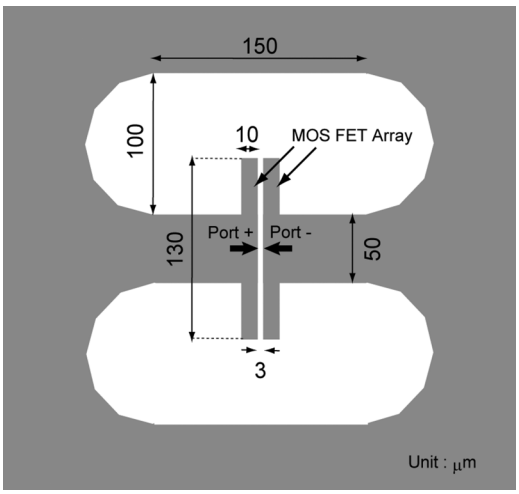

Fig. 2. Detailed shape of slots.

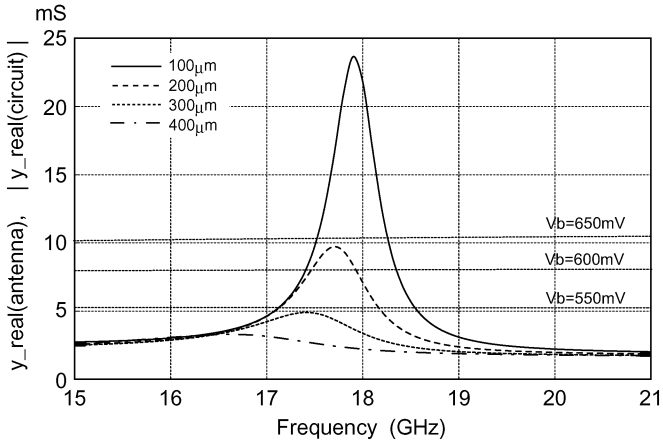

Fig. 3. Real parts of admittance.

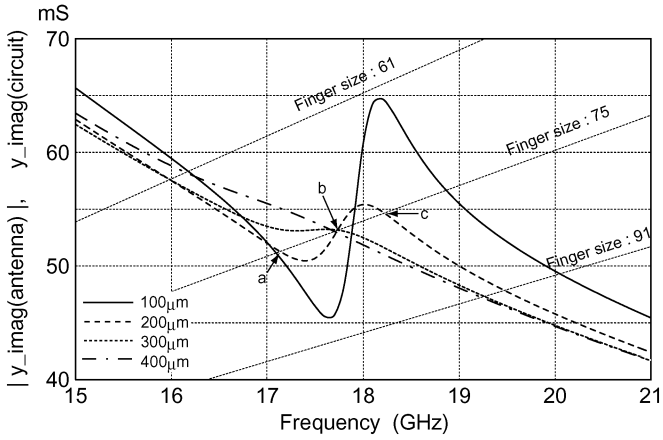

Fig. 4. Imaginary parts of admittance.

a result of the large parasitic capacitance. Hence, the low input impedance makes it difficult to implement a millimeter-wave radiation oscillator in standard CMOS technology.

B. Property of the Antenna

A high dielectric constant material (alumina 96%, $\varepsilon_r = 9.4$, $\tan\delta = 0.0004$) is used in the dielectric layer to reduce the patch size. The geometry of the microstrip patch antenna is also depicted in Figs. 1 and 2. The properties of the microstrip patch antenna were calculated by field simulation with Ansoft's HFSS. Figs. 3 and 4 show the input admittances of various thicknesses "h" of the dielectric layer. S11 has been evaluated on admittance, not impedance, with respect to the convenience of designing a cross-coupled CMOS oscillator, where the microstrip patch antenna is connected in parallel to cross-coupled CMOS FETs.

The real and imaginary parts of admittance are shown in Figs. 3 and 4, respectively. The real part at the resonant frequency becomes small as the thickness of the dielectric layer becomes large because the coupling between the patch and the slots becomes weak. On the other hand, the inflection in the imaginary part becomes large at the resonant frequency as the dielectric layer becomes thin. The efficiency of the antenna is shown in Fig. 5. Although the optimal thickness is 200 μm, the efficiency at a thickness of 300 μm is larger than 0.5, and

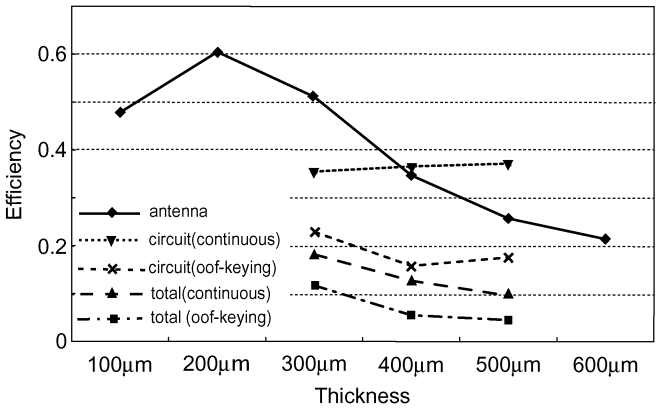

Fig. 5. Efficiencies of the antenna and the circuits.

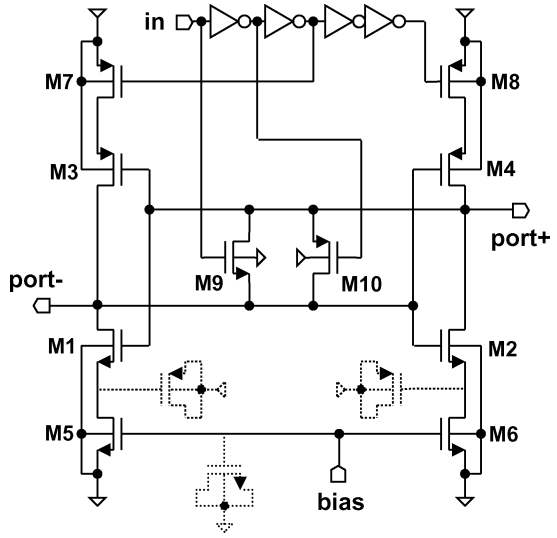

Fig. 6. Cross-coupling oscillator.

even the thickness at 400 μm has an efficiency of 0.35, which is sufficient for practical application, as shown in Fig. 5. The working frequencies at thicknesses of 300, 400, and 500 μm were 17.4, 16.5, and 16.2 GHz, respectively.

III. Oscillator Design

A. Oscillation Condition

Using the microstrip patch antenna as a resonator, a CMOS cross-coupling oscillator has been designed using 0.18-μm six-metal standard digital technology. The circuit schematic and the layout pattern are shown in Figs. 6 and 7, respectively. Here, M1–M4 form a cross-coupled transistor pair, and M5–M6 function as current sources. Because the drain currents of M1–M4 are equal to those of M5–M6 at the operation point, the bias voltage can tune the transconductance g_m of M1–M4 and the power consumption. In addition, M7–M10 and four inverters placed at the top are prepared for on/off-keying modulation. The MOS FETs indicated by dotted lines implement MOS capacitors that function as bypass capacitors. In addition, "port+" and "port−" are connected to the ports of the antenna described in Fig. 2.

In particular, the layout has been carefully designed so that both gate resistance and parasitic capacitance become small, as described in a previous study [7]. In standard CMOS technology, the gate material is polysilicon and its sheet resistance is relatively large. If the gate width is wide, the distance between the contact and the intrinsic MOS FET becomes large, and so the gate resistance cannot be ignored in high-frequency applications. On the other hand, if the gate width is too small, the number of fingers becomes very large to obtain sufficient transconductance, resulting in large line–line capacitances. Thus, optimization of the gate width (which is the finger width) is required for high-frequency applications, and the finger width of 0.89 μm is chosen as optimal.

As mentioned below, the number of fingers is varied as a parameter. Postcircuit simulations have been carried out after extracting the parasitic elements from the layout pattern. The admittances between "port+" and "port-" are shown in Figs. 3 and 4 together with the antenna properties. The real parts of various bias voltages are shown in Fig. 3, where the number of fingers is fixed at 75. Fig. 4 shows the imaginary parts of the various numbers of fingers. The property of the imaginary part changes only slightly with bias voltage, unlike the real part. The oscillation condition is given as

$$G_{\rm ant} + G_{\rm cir} < 0 \tag{1}$$

$$X_{\rm ant} + X_{\rm cir} = 0 \tag{2}$$

where $G_{\rm ant}$ and $G_{\rm cir}$ are the real parts of the admittances of the antenna and the cross-coupled pair, respectively, and $X_{\rm ant}$ and $X_{\rm cir}$ are the imaginary parts of the admittances of the antenna and the cross-coupled pair, respectively. Strictly speaking, (1) is the condition for oscillation to start. The condition for continuous oscillation ($G_{\rm ant} + G_{\rm cir} = 0$) is accomplished as a result of the nonlinearity of the MOSFET. Note that the real part of the cross-coupled pair and the imaginary part of the antenna are negative, whereas their absolute values are shown in Figs. 3 and 4. Note that $X_{\rm cir}$ is caused by parasitic capacitances, such as gate–source capacitance, and is approximately proportional to the number of fingers. The oscillator cannot operate with antennas having thicknesses of 100 or 200 μm considering the practical gain margin.

Even if a sufficiently large bias voltage ($>$ 750 mV) forcibly satisfies the gain condition of the 200-μm thickness, another obstacle arises with respect to the phase condition. As shown in Fig. 4, the imaginary curve intersects the cross-coupled pair with 75 fingers at three points: "a", "b", and "c". This means that these three frequencies satisfy the phase condition shown in (2). However, the oscillation is unstable at "b", and unfortunately, "b" is the resonant frequency of the patch antenna. The reason is probably that, rather than parallel resonance, the oscillation circuit has series resonance at "b". Although this phenomenon has been confirmed by circuit simulation (transient simulation), further analytical consideration is needed in the future.

B. On/Off Keying

To perform on/off-keying modulation, M7 and M8 are prepared, and the power supply is switched according to the input

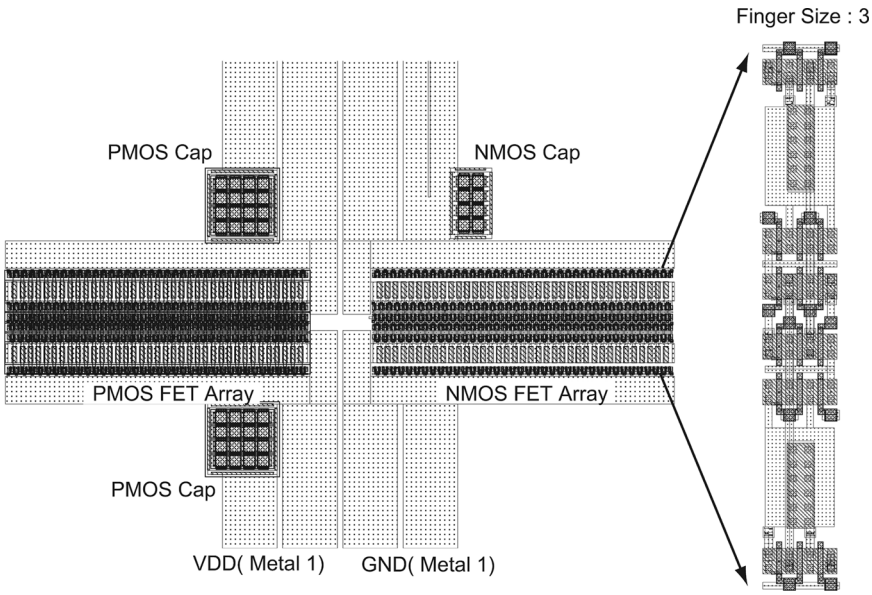

Fig. 7. Layout pattern.

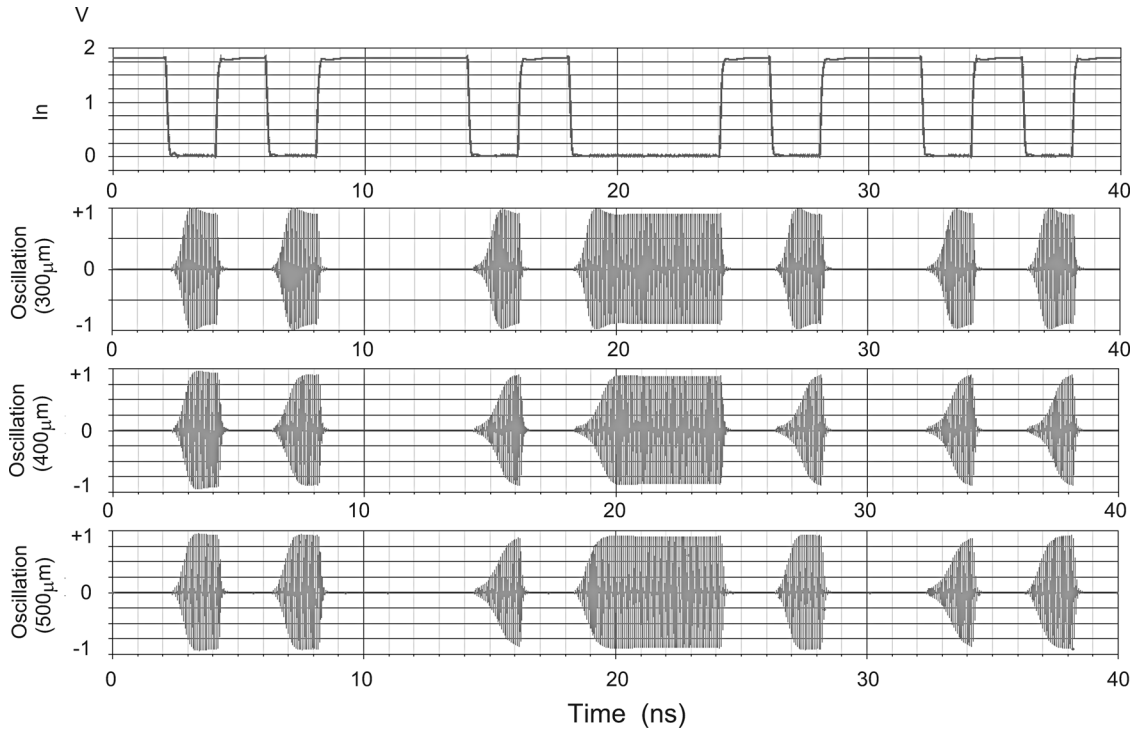

Fig. 8. Cross-coupling oscillator.

pulse. Note that two inverters shift the switch timing of M7 and M8, which slightly disturbs the balance between the left and right parts, which encourages vigorous oscillation. On the other hand, when the oscillation is stopped, the energy stored in the resonator (the antenna) is smoothly released by M9 and M10 shorting between "port+" and "port-". As shown in Fig. 8, the acceleration technique achieves a data rate of 500 Mb/s. Fig. 8 shows the transient simulation results for thicknesses of 300, 400, and 500 μm. The differential amplitude has been tuned to VDD ($= 1.8$ Vpp) by the bias voltage. The antenna was modeled as rational functions for time-domain simulation [8]. The parameters in the rational functions have been approximated from S-parameters calculated by an electromagnetic field solver.

The efficiencies of the circuit are shown in Fig. 5 together with the antenna property. An efficiency of over 0.35 can be realized for continuous oscillation but is reduced to 0.15–0.25 in the case of on/off keying. One reason for this is that the stored energy is released by M7 and M8 to realize a large data rate. The total efficiencies of the antenna and the circuit are also shown in Fig. 5. The radiation power can also be controlled by the Vbias condition for setting the oscillation. This has been confirmed

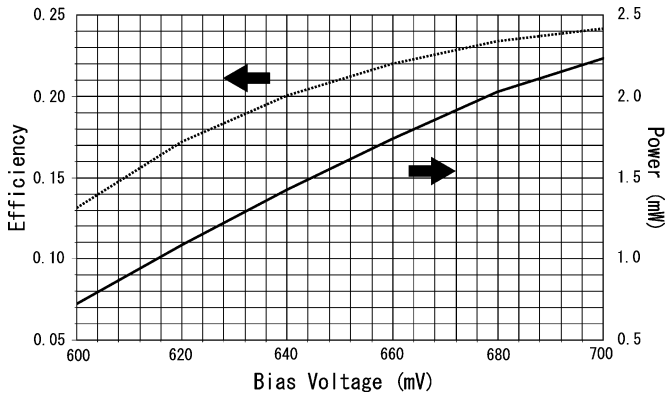

Fig. 9. Radiation power and efficiency.

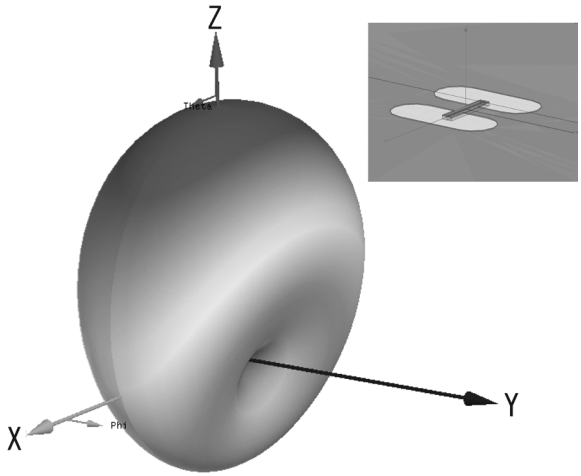

Fig. 10. Radiation pattern.

by SPICE simulation, as shown in Fig. 9, in the case of on/off keying with a thickness of 300 μm at 17.4 GHz.

IV. Discussion on Radiation Power

Radiation power is inversely proportional to the antenna impedance for a fixed amplitude voltage. The radiation power $P_{\rm rad}$ is expressed as

$$P_{\rm rad} = \frac{V_{\rm osc}^2}{R_{\rm ant}}\eta \tag{3}$$

where $V_{\rm osc}$, $R_{\rm ant}$, and η are the amplitude voltage (rms) of the oscillator, the input impedance, and the efficiency of the antenna, respectively. This may be disadvantageous in the above radiating oscillator because the oscillator contains a high-impedance antenna. Now, let us discuss the lower bound of the radiation power in short-range communication. The lower bound can be expressed as

$$P_{\rm rad} > \frac{P_{r(\min)}}{\left(\frac{1}{4\pi}\right)^2\left(\frac{\lambda}{r}\right)^2 G_l G_r} \tag{4}$$

where $P_{r(\min)}$ is the minimum receiving power, λ is the wavelength, r is the distance between the transmitter and the receiver, and G_t and G_r are the antenna gains of the transmitter and the receiver, respectively. For example, $P_{\rm rad} > -5.5$ dBm when $P_{r(\min)} = -60$ dBm, $\lambda = 1.67$ cm (18 GHz), $r = 100$ cm, and $G_t = G_r = 1.5$ dBi.

On the other hand, the radiation powers can be calculated as described in (3). Thus, the radiation powers at thicknesses of 300, 400, and 500 μm are calculated as 0.1, -3.4, and -5.3 dBm, respectively, from Figs. 1, 5, and 8. They satisfy the above condition for $P_{\rm rad} > -5.5$ dBm. The antenna gains at thicknesses of 300, 400, and 500 μm were 1.7, 1.6, and 1.5 dBi, respectively. The simulated radiation pattern at a thickness of 300 μm is shown in Fig. 10. The working frequency was 17.4 GHz.

V. Conclusion

A balanced electromagnetic coupling patch antenna has been proposed for direct connection to CMOS cross-coupling transistors, and a radiation oscillator has been implemented using the antenna. To satisfy the conditions of millimeter-wave oscillation, the parameters of the antenna and the cross-coupling transistor have been tuned by an electromagnetic field solver and postcircuit simulation after extracting the parasitic elements from the layout pattern.

Furthermore, employing switch transistors and two switching techniques has enabled the modulation of digital information by on/off keying, and the performance of 500 Mb/s and a total efficiency of 0.12 have been confirmed by circuit simulation.

The developments of a demodulation technique based on the proposed antenna and of a transceiver that is applicable to broadband short-range communication are subjects for future study.

References

[1] P. Russer, "Si and SiGe millimeter-wave integrated circuits," *IEEE Trans. Microw. Theory Tech.*, vol. 45, no. 5, pp. 590–603, May 1998.

[2] M. A. Dubois, J. F. Carpentier, P. Vincent, C. Billard, G. Parat, C. Muller, P. Ancey, and P. Conti, "Monolithic above-IC resonator technology for integrated architectures in mobile and wireless communication," *IEEE J. Solid-State Circuits*, vol. 41, no. 1, pp. 7–16, Jan. 2006.

[3] B. Otis, Y. H. Chee, and J. Rabaey, "A 400 μW-RX, 1.6 mW-TX super-regenerative transceiver for wireless sensor networks," in *Proc. ISSCC Dig. Tech. Papers*, Feb. 2005, pp. 396–397.

[4] B. Razzavi, "A 60 GHz CMOS receiver front-end," *IEEE J. Solid-State Circuits*, vol. 41, no. 1, pp. 17–22, Jan. 2006.

[5] M. D. Tsai, H. Wang, J. F. Kuan, and C. S. Chang, "A 70 GHz cascaded multi-stage distributed amplifier in 90 nm CMOS technology," in *Proc. ISSCC Dig. Tech. Papers*, Feb. 2005, pp. 402–403.

[6] T. Brauner, R. Vogt, and W. Bachtold, "A differential active patch antenna element for array applications," *IEEE Microw. Wireless Compon. Lett.*, vol. 13, no. 4, pp. 161–163, Apr. 2003.

[7] C. Cao and K. O. Kenneth, "A 90 GHz voltage-controlled oscillator with a 2.2 GHz tuning range in 130 nm CMOS technology," in *Proc. VLSI Circuits Dig. Tech. Papers Symp.*, Jun. 2005, pp. 242–243.

[8] C. P. Coelho, J. R. Phillips, and L. M. Silveira, "Robust rational function approximation algorithm for model generation," in *Proc. 36th Annu. DAC*, 1999, pp. 207–212.